

1 **Functional localization of the frontal eye fields in the common marmoset**  
2 **using microstimulation**

3 Janahan Selvanayagam<sup>1,3</sup>, Kevin D. Johnston<sup>2,3</sup>, David J. Schaeffer<sup>3</sup>, Lauren K. Hayrynen<sup>3</sup>,  
4 Stefan Everling<sup>1,2,3\*</sup>

5

6 <sup>1</sup> Graduate Program in Neuroscience, Western University, London, Ontario, Canada

7 <sup>2</sup> Department of Physiology and Pharmacology, Western University, London, Ontario, Canada

8 <sup>3</sup> Center for Functional and Metabolic Mapping, Robarts Research Institute, Western University,  
9 London, Ontario, Canada

10

11 **Author Contributions**

12 JS performed experiments, analysed data, prepared the figures, and wrote the first draft of the  
13 manuscript. KJ designed experiments, performed experiments, and edited the manuscript. DS  
14 analysed data and edited the manuscript. LH performed experiments and edited the manuscript.  
15 SE designed experiments, performed surgeries, edited the manuscript, and approved the final  
16 version of the manuscript.

17 **\* Corresponding author**

18 E-mail: [severlin@uwo.ca](mailto:severlin@uwo.ca), Centre for Functional and Metabolic Mapping, Robarts Research  
19 Institute, 1151 Richmond Street North, London, Ontario, N6A 5B7, Canada

20 **Number of pages:** 26

21 **Number of figures:** 8

22 **Number of words:** Abstract [249 WORDS], Significance statement [120 WORDS], Introduction  
23 [650 WORDS], Discussion [1313 WORDS]

## MICROSTIMULATION OF MARMOSET FRONTAL CORTEX

2

24

25 **Abstract**

26 The frontal eye field (FEF) is a critical region for the deployment of overt and covert spatial  
27 attention. While investigations in the macaque continue to provide insight into the neural  
28 underpinnings of the FEF, due to its location within a sulcus the macaque FEF is virtually  
29 inaccessible to electrophysiological techniques such as high-density and laminar recordings.  
30 With a largely lissencephalic cortex, the common marmoset (*Callithrix jacchus*) is a promising  
31 alternative primate model for studying FEF microcircuitry. Putative homologies have been  
32 established with the macaque FEF on the basis of cytoarchitecture and connectivity, however  
33 physiological investigation in awake, behaving marmosets is necessary to physiologically locate  
34 this area. Here we addressed this gap using intracortical microstimulation in a broad range of  
35 frontal cortical areas in marmosets. We implanted marmosets with 96-channel Utah arrays and  
36 applied microstimulation trains while they freely viewed video clips. We evoked short-latency  
37 fixed vector saccades at low currents (<50  $\mu$ A) in areas 45, 8aV, 8C and 6DR. We observed a  
38 topography of saccade direction and amplitude consistent with findings in macaques and  
39 humans; we observed small saccades in ventrolateral FEF and large saccades combined with  
40 contralateral neck and shoulder movements encoded in dorsomedial FEF. Our data provide  
41 compelling evidence supporting homology between marmoset and macaque FEF and suggest the  
42 marmoset is a useful primate model for investigating FEF microcircuitry and its contributions to  
43 oculomotor and cognitive functions.

44 **Keywords**

45 common marmoset; frontal cortex; frontal eye fields; saccade; microstimulation

46 **Significance Statement**

47 The frontal eye field (FEF) is a critical cortical region for overt and covert spatial attention. The  
48 microcircuitry of this area remains poorly understood, as in the macaque, the most commonly  
49 used model, it is embedded within a sulcus and is inaccessible to modern electrophysiological  
50 and optical imaging techniques. The common marmoset is a promising alternative primate  
51 model due to its lissencephalic cortex and potential for genetic manipulation. However,  
52 evidence for homologous cortical areas in this model remains limited and unclear. Here we  
53 applied microstimulation in frontal cortical areas in marmosets to physiologically identify the  
54 FEF. Our results provide compelling evidence for a frontal eye field in the marmoset, and  
55 suggest that the marmoset is a useful model for FEF microcircuitry.

56

## 57 **Introduction**

58 Described originally by Ferrier (1875) as a cortical area in macaque monkeys where  
59 electrical stimulation elicited contralateral eye and head movements, the frontal eye fields (FEF)  
60 in macaques and humans are now increasingly regarded as not only a motor area for saccades  
61 and head movements, but also as a critical region for the deployment of overt and covert spatial  
62 attention (Awh et al., 2006). Over the past 40 years, most of our knowledge regarding the neural  
63 processes in the FEF has come from experiments in awake behaving macaque monkeys. In these  
64 Old-World primates, FEF is defined as an area within the rostral bank and fundus of the arcuate  
65 sulcus from which electrical microstimulation evokes saccades at low currents ( $<50 \mu\text{A}$ ) (Bruce  
66 et al., 1985). Stimulation, recording, and pharmacological manipulation studies in trained  
67 macaque monkeys have and continue to provide critical insights into the neural processes in FEF  
68 that underlie saccade control and visual attention. However, the local FEF microcircuitry remains  
69 poorly understood as, due to its location within a sulcus, macaque FEF is virtually inaccessible to  
70 intralaminar recordings and manipulations.

71 The New-World common marmoset (*Callithrix jacchus*) is a promising alternative  
72 primate model for studying FEF microcircuitry. These small primates have a largely  
73 lissencephalic cortex and can be trained to perform saccadic eye movement tasks head-restrained  
74 (Mitchell et al., 2014; Johnston et al., 2018, 2019). A first step towards such experiments is the  
75 physiological identification of the FEF in marmosets. Existing evidence for the location of this  
76 area in this species, however, remains limited and unclear. An early marmoset study by Mott  
77 and colleagues (1910) reported that both eye and combined eye and head movements could be  
78 evoked by electrical stimulation at several frontal cortical sites. Subsequently, Blum and  
79 colleagues (1982) confirmed and extended these earlier results. They observed movements

80 including ipsilateral and contralateral saccades, eye movements in all directions, and slow  
81 drifting movements. It seems that these eye movements were evoked in areas 6DC, 6DR, 8aD,  
82 and 46 with no clear topography of direction or amplitude. Interpretation of these earlier studies  
83 is difficult, however, as the anesthetized preparations used most likely influenced the properties  
84 of the eye movements evoked (Robinson and Fuchs, 1969).

85 More recently, anatomical evidence has suggested that marmoset FEF lies within areas  
86 45 and 8aV (Reser et al., 2013). Both areas have widespread connections with extrastriate visual  
87 areas, and areas labelled FEF and FV by Collins et al (2005), which may correspond to areas 45  
88 and 8aV, contain clusters of neurons projecting to the SC, an area critical for the initiation of  
89 saccadic and orienting movements. Area 8aV in marmosets also contains large layer V pyramidal  
90 neurons, a cytoarchitectonic characteristic of macaque FEF (Stanton et al., 1989). Consistent  
91 with this notion, fMRI studies in marmosets have reported BOLD activation in areas 45 and 8aV  
92 in response to visual stimuli (Hung et al., 2015), though a resting-state fMRI functional  
93 connectivity study found the strongest SC connectivity in area 8aD, at the border of area 6DR  
94 (Ghahremani et al., 2017). The authors proposed that this region either corresponded to the  
95 marmoset FEF or that it may encode large amplitude saccades, while area 8aV may encode small  
96 amplitude saccades.

97 Here, we set out to physiologically identify the marmoset FEF using the classical  
98 approach of intracortical electrical microstimulation (ICMS). We applied microstimulation trains  
99 via chronically implanted 96-channel electrode arrays placed to target a broad range of frontal  
100 cortical areas in three awake marmosets. Our findings revealed a topography of contralateral  
101 saccade amplitude in marmoset frontal cortex similar to that observed in macaques (Bruce et al.,  
102 1985; Schall, 1997) and humans (Foerster, 1926), with small saccades being encoded in area 45

103 and lateral parts of area 8aV, and larger saccades combined with contralateral neck and shoulder  
104 movements encoded in the medial posterior portion of area 8aV, area 8C, and area 6DR.

## 105 **Methods**

### 106 **Subjects**

107 We obtained data from 3 adult common marmosets (*Callithrix jacchus*; M1 male, 17  
108 months; M2 female 20 months; M3 male 23 months). All experimental procedures conducted  
109 were in accordance with the Canadian Council of Animal Care policy on the care and use of  
110 laboratory animals and a protocol approved by the Animal Care Committee of the University of  
111 Western Ontario Council on Animal Care. The animals were under the close supervision of  
112 university veterinarians.

113 Prior to the commencement of microstimulation experiments, each animal was  
114 acclimated to restraint in a custom primate chair (Johnston et al., 2018). Animals then  
115 underwent an aseptic surgical procedure under general anesthesia in which 96 channel Utah  
116 arrays (4mm x 4mm; 1mm electrode length; 400µm pitch; iridium oxide tips) were implanted in  
117 left frontal cortex. During this surgery, a microdrill was used to initially open 4mm burr holes in  
118 the skull and were enlarged as necessary using a rongeur. Arrays were manually inserted; wires  
119 and connectors were fixed to the skull using dental adhesive (Bisco All-Bond, Bisco Dental  
120 Products, Richmond, BC, Canada). Once implanted, the array site was covered with silicone  
121 adhesive to seal the burr hole (Kwik Sil, World Precision Instruments, Sarasota, FLA, USA). A  
122 screw-hole was drilled into the skull on the opposite side to the location of the implanted array to  
123 place the ground screw. The ground wire of the array was then tightly wound around the base of  
124 the screw to ensure good electrical connection. A combination recording chamber/head holder

125 (Johnston et al., 2018) was placed around the array and connectors and fixed in place using  
126 further layers of dental adhesive. Finally, a removable protective cap was placed on the chamber.

### 127 **Localizing the array**

128 To precisely determine array locations, high-resolution T2-weighted structural magnetic  
129 resonance images (MRI; obtained pre-surgery) were co-registered with computerized  
130 tomography (CT) scans (obtained post-surgery). The MRI images provided each marmoset's  
131 brain geometry with reference to the location of the skull, while the CT images allowed for  
132 localization of the skull and the array boundaries. By co-registering the skulls across the two  
133 modalities, the precise array-to-brain location was determined for each animal.

134 Pre-surgical MRIs were acquired using an 9.4 T 31 cm horizontal bore magnet  
135 (Varian/Agilent, Yarnton, UK) and Bruker BioSpec Avance III console with the software  
136 package Paravision-6 (Bruker BioSpin Corp, Billerica, MA) and a custom-built high  
137 performance 15-cm-diameter gradient coil with 400-mT/m maximum gradient strength (xMR,  
138 London, CAN; Peterson et al., 2018). A geometrically optimized 8-channel phased array receive  
139 coil was designed in-house, for SNR improvement and to allow for acceleration of the echo  
140 planar imaging of marmoset cohorts (Gilbert et al., 2019). Preamplifiers were located behind the  
141 animal and the receive coil was placed inside a quadrature birdcage coil (12-cm inner diameter)  
142 used for transmission. Prior to each imaging session, anesthesia was induced with ketamine  
143 hydrochloride at 20 mg/kg. During scanning, marmosets were anesthetized with isoflurane and  
144 maintained at a level of 2% throughout the scan by means of inhalation. Oxygen flow rate was  
145 kept between 1.75 and 2.25 l/min throughout the scan. Respiration, SpO<sub>2</sub>, and heart rate were  
146 continuously monitored and were observed to be within the normal range throughout the scans.  
147 Body temperature was also measured and recorded throughout, maintained using warm water



148 circulating blankets, thermal insulation, and warmed air. All animals were head-fixed in  
149 stereotactic position using a custom-built MRI bed with ear bars, eye bars, and a palate bar  
150 housed within the anesthesia mask (Gilbert et al., 2019). All imaging was performed at the  
151 Centre for Functional and Metabolic Mapping at the University of Western Ontario. T2-weighted  
152 structural scans were acquired for each animal with the following parameters: TR = 5500 ms, TE  
153 = 53 ms, field of view =  $51.2 \times 51.2$  mm, matrix size =  $384 \times 384$ , voxel size =  $0.133 \times 0.133 \times$   
154  $0.5$  mm, slices = 42, bandwidth = 50 kHz, GRAPPA acceleration factor: 2.

155 CT scans were obtained on a micro-CT scanner (eXplore Locus Ultra, GR Healthcare  
156 Biosciences, London, ON) after array implantation. Prior to the scan, marmosets were  
157 anesthetized with 15mg/kg Ketamine mixed with 0.025mg/kg Medetomidine. X-ray tube  
158 potential of 120 kV and tube current of 20 mA were used for the scan, with the data acquired at  
159  $0.5^\circ$  angular increment over  $360^\circ$ , resulting in 1000 views. The resulting CT images were then  
160 reconstructed into 3D with isotropic voxel size of 0.154 mm. Heart rate and SpO2 were  
161 monitored throughout the session. At the end of the scan, the injectable anesthetic was reversed  
162 with an IM injection of 0.025mg/kg Ceptor.

163 The raw MRI and CT images were converted to NifTI format using dcm2niix (Li et al.,  
164 2016) and the MRIs were reoriented from the sphinx position using FSL software (Smith et al.,  
165 2004). Then, using FSL (FSLeyes nudge function), each animal's CT image was manually  
166 aligned to their MRI image based on the skull location – this allowed for co-localization of the  
167 array and brain surface. The array position from the CT image was determined by a hyper-  
168 intensity concomitant with the metallic contacts contained within the array; this hyper-intensity  
169 stood out against the lower intensities of the skull and surrounding tissues. A region of interest  
170 (ROI) was manually drawn within the array location for each animal to be displayed on the NIH

171 marmoset brain atlas surface (Liu et al., 2018) for ease of viewing. The NIH marmoset brain  
172 atlas is an ultra-high resolution *ex vivo* MRI image dataset that contains the locations of  
173 cytoarchitectonic boundaries (Liu et al., 2018). As such, to determine the array location with  
174 reference to the cytoarchitectonic boundaries, we non-linearly registered the NIH template brain  
175 to each marmoset's T2-weighted image using Advanced Normalization Tools (ANTs; Avants et  
176 al., 2011) software. The resultant transformation matrices were then applied to the  
177 cytoarchitectonic boundary image included with the NIH template brain atlas. The olfactory bulb  
178 was manually removed from the marmoset T2-weighted image of each animal prior to  
179 registration, as it was not included in the template image. As a result of the transformations, the  
180 template brain surface, the cytoarchitectonic boundaries, and the array location (ROI described  
181 above) could be rendered on each animals' individual native-space brain surface.

## 182 **Data collection**

183       Following recovery, we verified that electrode contacts were within the cortex by  
184 monitoring extracellular neural activity using the Open Ephys acquisition board  
185 (<http://www.open-ephys.org>) and digital headstages (Intan Technologies, Los Angeles, CA,  
186 USA). Upon observing single or multiunit activity at multiple sites in the array, we commenced  
187 microstimulation experiments.

188       Animals were head restrained in a custom primate chair (Johnston et al., 2018) mounted  
189 on a table in a sound attenuating chamber (Crist Instruments Co., Hagerstown, MD, USA). A  
190 spout was placed at the monkey's mouth to deliver a viscous preferred reward of acacia gum.  
191 This was delivered via infusion pump (Model NE-510, New Era Pump Systems, Inc.,  
192 Farmingdale, New York, USA). In each session, eye position was calibrated by rewarding 300  
193 to 600ms fixations on a marmoset face presented at one of five locations on the display monitor

194 using the CORTEX real-time operating system (NIMH, Bethesda, MD, USA). Faces were  
195 presented at the display centre, at 6 degrees to the right and left of centre, and at 6 degrees  
196 directly above and below centre. All stimuli were presented on a CRT monitor (ViewSonic  
197 Optiquest Q115, 76 Hz non-interlaced, 1600 x 1280 resolution).

198 Monkeys freely viewed short repeating video clips to sustain their alertness while we  
199 applied manually triggered microstimulation trains. Monkeys were intermittently rewarded at  
200 random time intervals to maintain their interest. Microstimulation trains were delivered using  
201 the Intan RHS2000 Stimulation/Recording Controller system and digital stimulation/recording  
202 headstages (Intan Technologies, Los Angeles, CA, USA). Stimulation trains consisted of 0.2-  
203 0.3ms biphasic current pulses delivered at 300 Hz for a duration of 100-400ms, at current  
204 amplitudes varying between 5 and 300  $\mu$ A. At sites where skeletomotor or saccadic responses  
205 were evoked, we carried out a current series to determine thresholds. The threshold was defined  
206 as the minimum current at which a given response was evoked on 50% of stimulation trials.  
207 Skeletomotor responses were observed manually by researchers. Eye position was digitally  
208 recorded at 1 kHz via video tracking of the left pupil (EyeLink 1000, SR Research, Ottawa, ON,  
209 Canada).

## 210 **Data analysis**

211 Analysis was performed with custom python code. Eye velocity (visual deg/s) was  
212 obtained by smoothing and numerical differentiation. Saccades were defined as horizontal or  
213 vertical eye velocity exceeding 30 deg/s. Blinks were defined as the radial eye velocity  
214 exceeding 1500 deg/s.

215 As we did not require marmosets to fixate during stimulation, saccades following  
216 stimulation could be spontaneous. A bootstrap analysis was used to quantitatively determine if

217 saccades were more probable following stimulation than at any other time during a session. In a  
218 single session, 60-80 trains were delivered at a single site holding stimulation parameters  
219 constant over a 2-minute period. Stimulation onset times were shuffled (time points were  
220 randomly sampled without replacement with millisecond resolution over the duration of the  
221 session) and the probability of a saccade occurring in a 200ms window following the selected  
222 timepoints was computed. This was repeated 1000 times for each session to obtain a distribution  
223 of probabilities of saccade occurrence. The percentile rank of the probability of stimulation  
224 evoking a saccade with respect to this distribution was computed; the 95th percentile marked the  
225 5% significance criterion indicating a session where stimulation significantly increased the  
226 probability of saccade occurrence.

## 227 **Results**

### 228 **Evoked skeletomotor and oculomotor responses**

229         Array locations were confirmed using CT scans obtained after the surgery, which were  
230 co-registered with MR scans obtained before the surgery (see Fig. 1a). Microstimulation was  
231 conducted at 288 sites across 3 marmosets. We observed a range of skeletomotor and  
232 oculomotor responses across the frontal cortex (Fig. 1b, c).

233         At the most posterior sites, we observed primarily single joint movements with a gross  
234 medio-lateral topography. We observed hindlimb movements (leg, foot, toes) most medially,  
235 followed by forelimb (arm, hand, finger) and facial movements (eyelid, ear, nose, jaw) most  
236 laterally - an organization characteristic of primary motor cortex (area 4) (Burish et al., 2008;  
237 Wakabayashi et al., 2018). Anterior to this, we observed overlapping representation of forelimb,

238 facial, shoulder, and neck musculature with no obvious organization, similar to that observed in  
239 the marmoset premotor cortex (area 6) (Burish et al., 2008; c.f. Wakabayashi et al., 2018).

240 We elicited saccades at 61 sites across 3 marmosets (see Fig. 1c). At 6 sites on the border  
241 of area 6DC and 6M, we observed goal directed saccades characteristic of the supplementary eye  
242 fields (SEF), albeit at long latencies (70-110ms) and high currents (200  $\mu$ A) (see Fig. 3a). At 3  
243 sites in area 46D and the anterior portion of area 8aD, we elicited saccades with no clear pattern  
244 at long latencies (75-90ms) and high currents (300  $\mu$ A) (see Fig. 3b). Saccades evoked from  
245 these sites were mostly directed to the hemifield contralateral to the stimulated site, though some  
246 saccades directed to the ipsilateral hemifield were observed.

247 We elicited fixed vector saccades at 52 sites across areas 6DR, 8C, 8aV and 45. Mean  
248 saccade vectors are plotted in Fig. 1c. Representative saccade traces are plotted in Fig. 2. In  
249 areas 6DR, 8C and the medial portion of 8aV, we observed larger saccades often coupled with  
250 shoulder, neck, and ear movements with the most common response being a shoulder rotation  
251 that resembled orienting towards contralateral side. In area 45 and the lateral portion of area 8aV,  
252 we observed smaller saccades with no visible skeletomotor responses. Smooth eye movements  
253 could be elicited at 5 sites in areas 6DR and 8C.

#### 254 **Saccade thresholds and latencies**

255 At sites where we observed fixed vector saccades, we conducted current series to  
256 determine thresholds and characterize any current-related changes in saccade metrics. Current  
257 series from five representative sites are shown in Fig. 4a-e. Thresholds were defined as the  
258 minimum current at which saccades could be evoked 50% of the time (see Fig. 4g). Thresholds  
259 ranged from 12-300  $\mu$ A. Saccades were evoked at low thresholds (<50  $\mu$ A) at 35 of the 52 sites

260 from which we were able to evoke fixed vector saccades (see Fig. 1d). Saccade metrics were  
261 computed at the minimum current at which saccades could be evoked 75% of the time.

262 Each site had a stereotypical saccade latency, though we found no systematic variation in  
263 saccade latency with respect to site coordinates nor any other saccade metrics. Saccade latencies  
264 ranged from 25-85ms, with the majority falling in the range between 40-60ms (see Fig. 4h).  
265 Saccade latencies were generally longer and more variable near the current threshold for a given  
266 site. When using high currents well above threshold (200-300  $\mu$ A), uniformly short saccade  
267 latencies were observed (15-45ms).

### 268 **Topography of evoked saccades**

269 Evoked saccades were directed contralateral to the stimulated hemisphere and mostly  
270 fixed vector (see Fig 1c, Fig 2, Fig 4a-e), exhibiting relatively consistent directions and  
271 amplitudes independent of the initial eye position. Although we did not systematically vary  
272 initial eye positions, the fact that marmosets were allowed to freely direct their gaze across video  
273 clips on the display monitor during experimental sessions ensured a wide range of initial eye  
274 positions at the time of microstimulation onset. Most initial eye positions fell within a 13 degree  
275 range similar to observations elsewhere in marmosets (Mitchell et al., 2014) and other New  
276 World monkeys (Heiney and Blazquez, 2011). 90% of initial eye positions fell within the  
277 following ranges for each marmoset: Marmoset 1: -13.6 to 12.4 abscissa, -10.7 to 11.4 ordinate;  
278 Marmoset 2: -12.7 to 15.7 abscissa, -11.7 to 9.6 ordinate; Marmoset 3: -12.9 to 12.7 abscissa, -  
279 18.5 to 14.3 ordinate. Amplitude decreased progressively from medial (large saccades; >20  
280 visual degrees) to lateral (small saccades; <2 visual degrees) sites. Direction varied  
281 systematically from upper visual field at posterior medial sites to lower visual field at anterior  
282 lateral sites.

283 **Staircase saccades**

284           At a subset of sites from which saccades were evoked, we additionally observed  
285 staircases of multiple saccades. To investigate this further, we applied stimulation trains of  
286 increasing duration at these sites and found that the number of saccades increased as a function  
287 of train duration at the majority of these sites (12/15). A representative site is depicted in Fig. 5.  
288 Staircases consisted of 2-5 consecutive saccades with consistent amplitudes and directions, in  
289 many cases ultimately driving the eye to the extent of its oculomotor range. At a given site,  
290 consecutive saccades occurred at fixed intervals. The intersaccadic interval ranged from 70-120  
291 ms across sites and we observed no systematic variation in intersaccadic interval with respect to  
292 site coordinates nor any other saccade metrics.

293 **Smooth eye movements**

294           Posterior to where we evoked saccades, in areas 6DR and 8C (see Fig. 1c), we were able  
295 to elicit smooth eye movements. These eye movements often followed a saccade and continued  
296 until stimulation ended at which point, they stopped abruptly (see Fig. 6a for a representative  
297 site). While the direction of these movements was consistent at a site, the velocity increased as a  
298 function of stimulation current intensity, consistent with what is observed in the smooth pursuit  
299 region of the FEF in macaques (see Fig. 6b for a current series at a representative site) (Gottlieb  
300 et al., 1993).

301 **Effects of initial gaze position**

302           While evoked saccades were mostly fixed vector, an effect of initial gaze position was  
303 observed at some sites. At those sites, saccades tended to be of greater amplitude if the gaze  
304 position at the time of stimulus onset was within the hemifield ipsilateral to the stimulated

305 hemisphere. Further, the probability of evoking a saccade was lower if the initial eye position  
306 was within the hemifield contralateral to the stimulated hemisphere.

307         We quantified the magnitude of the effect of initial eye position at each site by computing  
308 the linear regression of the difference in final eye position as a function of the initial eye position  
309 separately for horizontal ( $K_h$ ) and vertical ( $K_v$ ) components of evoked saccades at these sites  
310 (Russo and Bruce, 1993). Correlation coefficients of 0 would be expected for sites at which the  
311 saccade vector did not change with varying initial eye positions (i.e. strictly fixed-vector  
312 saccades), whereas coefficients of -1 would be expected for sites at which evoked saccades  
313 terminated at the same eye position irrespective of initial eye position (i.e. goal-directed  
314 saccades). An example of this is shown for representative sites from FEF (see Fig. 6a, b) and  
315 SEF (see Fig. 6c).

316         Sites in FEF were mostly fixed vector, however, as observed by Russo and Bruce (1993),  
317 the effect of initial eye position increases in magnitude with the mean amplitude of saccades  
318 evoked at that site (see Fig. 6d). This corresponds with the eye position terminating at the edge  
319 of the orbit for very large saccades. In contrast, in SEF sites, mostly convergent saccades were  
320 observed with correlation coefficients close to -1 and saccades converging on locations well  
321 within the oculomotor range of the animal.

## 322 **Discussion**

323         The common marmoset is a promising model for investigating the microcircuitry of the  
324 FEF (Mitchell and Leopold, 2015). The location of the FEF in marmosets, however, remains  
325 controversial. To address this, we systematically applied intracortical microstimulation (ICMS)  
326 to marmoset frontal cortex through chronically implanted electrode arrays to investigate the



327 oculomotor and skeletomotor responses evoked in this region (see Fig. 7 for a schematic  
328 summary). We observed patterns of skeletomotor responses consistent with previous ICMS  
329 investigations of marmoset motor and premotor cortex (Burish et al., 2008; Wakabayashi et al.,  
330 2018). Anterior to these motor areas, we observed a suite of oculomotor responses across  
331 frontal cortex which we propose correspond to three cortical eye fields. ICMS in area 45 and in  
332 the lateral part of area 8aD evoked small contraversive saccades at very low currents, consistent  
333 with the properties of the ventrolateral FEF (vFEF) in macaques (Bruce et al. 1985). In areas  
334 6DR, 6DC, 8C, and medial 8aV, ICMS evoked larger saccades that were often associated with  
335 shoulder, neck and ear movements. This is consistent with ICMS experiments in dorsomedial  
336 macaque FEF (dFEF) (Elsley et al., 2007; Corneil et al., 2010). We also observed goal-oriented  
337 saccades characteristic of the supplementary eye field (SEF) at dorsomedial sites. In prefrontal  
338 areas 46 and anterior 8aD, ICMS elicited saccades with no consistent organization of direction or  
339 amplitude. These findings are consistent with the organization of FEF and SEF in macaques  
340 (Robinson and Fuchs, 1969; Bruce et al., 1985; Schlag and Schlag-Rey, 1987; Gottlieb et al.,  
341 1993; Russo and Bruce, 1993; Knight and Fuchs, 2007).

342 A characteristic feature of the FEF observed in macaque ICMS experiments is the ability  
343 to evoke short latency fixed vector saccades at low currents. While the threshold to evoke  
344 saccades can be as high as 2 mA in frontal cortex (Robinson and Fuchs, 1969), FEF is defined in  
345 macaque as the restricted region in which thresholds are below 50  $\mu$ A (Bruce et al., 1985). Here,  
346 we observed a large number of sites with thresholds below 50  $\mu$ A, with a lower bound of 12  $\mu$ A,  
347 similar to the 10  $\mu$ A observed in macaque (Bruce et al., 1985). This is despite the limitations of  
348 fixed-length chronic electrode arrays which did not allow us optimally target layer V output  
349 neurons and in contrast to previous reports of higher thresholds in marmoset motor cortex

350 compared to macaques (Burish et al., 2008). However, saccade latencies were slightly longer  
351 than those observed in macaques. We found a range of 25-85ms as compared to 20-60ms  
352 observed by Bruce and colleagues (1985) at near threshold currents, and 15-45ms as compared to  
353 15-25ms by Robinson and Fuchs (1969) at higher currents. It has been proposed that longer  
354 latency saccades are evoked through an indirect route (e.g., superior colliculus), whereas shorter  
355 latency saccades are evoked by recruiting neurons that project directly to the brain stem (Bruce  
356 et al., 1985). Investigations employing single unit recordings in the marmoset FEF and studies  
357 investigating the connectivity of marmoset FEF and brain stem oculomotor nuclei should provide  
358 insight into these differences.

359         In macaque FEF, saccades evoked by ICMS are fixed-vector with little variability in  
360 amplitude and direction (Robinson and Fuchs, 1969; Bruce et al., 1985). While saccades evoked  
361 here were predominantly fixed vector, some effects of initial gaze position were observed in  
362 which saccades were larger when the initial gaze position was in the hemifield ipsilateral to the  
363 site of stimulation. Similar observations have been made in macaque FEF (Robinson and Fuchs,  
364 1969; Russo and Bruce, 1993) in which the magnitude of this effect is greater for larger  
365 saccades. However, this effect is greater here than previously observed with macaques. This may  
366 be a result of the eye being driven to the edge of the oculomotor range. In marmosets, this is  
367 limited to approximately 12 degrees as compared to 30 degrees in the macaque (Tomlinson and  
368 Bahra, 1986; Heiney and Blazquez, 2011; Mitchell et al., 2014). Head-restraint also prevents  
369 marmosets from using head movements to shift gaze, which they depend on to a greater extent  
370 than larger primates (Mitchell et al., 2014). Investigations in head unrestrained marmosets  
371 would clarify these differences.

372         Previous studies of macaque FEF have revealed a topographic representation of saccade

373 amplitude and direction. Bruce and colleagues (1985) demonstrated a medio-lateral gradient in  
374 which large saccades were evoked medially and small saccades laterally. We observed a similar  
375 organization of saccade amplitude in marmosets, with small saccades being elicited in areas 45  
376 and lateral area 8aV (vFEF) and larger saccades being evoked in areas 6DR, 6C, 8C, and medial  
377 8aV (dFEF). Bruce and colleagues (1985) observed systematic changes in saccade direction with  
378 small advances along the depth of the arcuate sulcus in macaques, though they often encountered  
379 disruptions and reversals of direction. We observed a rostro-caudal organization of saccade  
380 direction in marmosets in which direction gradually changed from lower to upper visual field,  
381 though there were occasional direction reversals. Assuming that frontal cortex in marmoset is  
382 roughly a flattened version of that in macaque, the rostro-caudal axis would correspond roughly  
383 to traversing the depth of the arcuate sulcus from lip to fundus in macaques. We additionally  
384 observed a more continuous medio-lateral organization of saccade direction, such that the upper  
385 visual field was represented medially. This organization would be difficult to observe in the  
386 macaque FEF due to its more complex morphology.

387         At more posterior-medial sites where larger saccades are represented (dFEF), we  
388 observed skeletomotor responses resembling an orienting response while we only observed  
389 oculomotor responses at the more anterior-lateral sites. This is in line with what Knight and  
390 Fuchs (2007) found in awake head-unrestrained macaques. Indeed, Foerster (1926) already  
391 reported two saccade-related fields in humans: (1) FEF where epileptic seizures evoked  
392 contralateral saccades and (2) a more posterior field that he termed frontal adversive field  
393 (frontales Adversivsfeld) where seizures were associated with contralateral saccades and head  
394 movements.

395         At posterior medial sites, at the border of area 6D and 6M, we observed goal-directed

396 saccades characteristic of SEF (Schlag and Schlag-Rey, 1987). Contrary to observations at more  
397 anterior lateral sites, convergence of saccades could not be explained by physical limitation of  
398 the orbit. We observed saccades converging at locations well within the animal's oculomotor  
399 range and, albeit infrequently, saccades directed to the hemifield ipsilateral to the stimulated  
400 hemisphere. These findings are similar to observations in the macaque by Schlag and Schlag-  
401 Rey (1987). However, we observed that saccade latencies were much longer at these sites (70-  
402 110ms) than those observed by Schlag and Schlag-Rey (1987) (40-60ms). Further, they  
403 observed low current thresholds, at many sites less than 20  $\mu$ A, whereas we observed few  
404 saccades at currents as high as 200  $\mu$ A. Taken together, these findings suggest the observed  
405 responses may be evoked due to current spread to dorsomedial regions not covered by our arrays.  
406 We propose that area 6M may contain the putative marmoset SEF. Further investigation  
407 employing ICMS and single unit electrophysiology in marmoset dorsomedial frontal cortex is  
408 required to fully investigate this putative homology.

409         We were also able to elicit saccades at rostral sites in area 46 and in anterior area 8aD.  
410 At these sites, saccades were evoked at high currents and long latencies, and did not exhibit any  
411 clear organization of direction or amplitude. As with our observations in other areas of marmoset  
412 frontal cortex, this finding is consonant with previous work in macaque (Robinson and Fuchs,  
413 1969). Further investigation in the frontal pole of the marmoset brain is required to characterize  
414 this region.

415         Altogether, our data demonstrate a similar functional organization of the FEF in  
416 marmosets and macaques and provide a combined physiological characterization and anatomical  
417 localization that opens avenues for future exploration of FEF microcircuitry in marmosets.  
418 Electrophysiological studies in marmosets have the potential to complement ongoing work in the

## MICROSTIMULATION OF MARMOSET FRONTAL CORTEX

21

419 macaque model and human participants by advancing our understanding of laminar processes

420 and their contributions to the oculomotor and cognitive functions of this area.

421

422 **Acknowledgements**

423           We thank C. Vander Tuin, N. Hague, W. Froese, and K. Faubert for expert technical and  
424 surgical assistance, and care of the marmosets. This research was supported by the Canadian  
425 Institutes of Health Research grant FRN148365 to S.E. and the Canada First Research  
426 Excellence Fund to BrainsCAN.

427 **References**

- 428 Avants BB, Tustison NJ, Song G, Cook PA, Klein A, Gee JC (2011) A Reproducible Evaluation  
429 of ANTs Similarity Metric Performance in Brain Image Registration. *NeuroImage*  
430 54:2033–2044.
- 431 Awh E, Armstrong KM, Moore T (2006) Visual and oculomotor selection: links, causes and  
432 implications for spatial attention. *Trends Cogn Sci* 10:124–130.
- 433 Blum B, Kulikowski JJ, Carden D, Harwood D (1982) Eye Movements Induced by Electrical  
434 Stimulation of the Frontal Eye Fields of Marmosets and Squirrel Monkeys. *Brain Behav*  
435 *Evol* 21:34–41.
- 436 Bruce CJ, Goldberg ME, Bushnell MC, Stanton GB (1985) Primate frontal eye fields. II.  
437 Physiological and anatomical correlates of electrically evoked eye movements. *J*  
438 *Neurophysiol* 54:714–734.
- 439 Burish MJ, Stepniewska I, Kaas JH (2008) Microstimulation and architectonics of frontoparietal  
440 cortex in common marmosets (*Callithrix jacchus*). *J Comp Neurol* 507:1151–1168.
- 441 Corneil BD, Elsley JK, Nagy B, Cushing SL (2010) Motor output evoked by subsaccadic  
442 stimulation of primate frontal eye fields. *Proc Natl Acad Sci U S A* 107:6070–6075.
- 443 Elsley JK, Nagy B, Cushing SL, Corneil BD (2007) Widespread Presaccadic Recruitment of  
444 Neck Muscles by Stimulation of the Primate Frontal Eye Fields. *J Neurophysiol*  
445 98:1333–1354.
- 446 Ferrier D (1875) The Croonian Lecture: Experiments on the Brain of Monkeys (second series).  
447 *Philosophical Trans R Soc Lond* 165:433–488.
- 448 Foerster O (1926) Zur operativen Behandlung der Epilepsie. *Dtsch Z Für Nervenheilkd* 89:137–  
449 147.

- 450 Ghahremani M, Hutchison RM, Menon RS, Everling S (2017) Frontoparietal Functional  
451 Connectivity in the Common Marmoset. *Cereb Cortex* 27:3890–3905.
- 452 Gilbert KM, Schaeffer DJ, Gati JS, Klassen ML, Everling S, Menon RS (2019) Open-source  
453 hardware designs for MRI of mice, rats, and marmosets: Integrated animal holders and  
454 radiofrequency coils. *J Neurosci Methods* 312:65–72.
- 455 Gottlieb JP, Bruce CJ, MacAvoy MG (1993) Smooth eye movements elicited by  
456 microstimulation in the primate frontal eye field. *J Neurophysiol* 69:786–799.
- 457 Heiney SA, Blazquez PM (2011) Behavioral responses of trained squirrel and rhesus monkeys  
458 during oculomotor tasks. *Exp Brain Res* 212:409–416.
- 459 Hung C-C, Yen CC, Ciuchta JL, Papoti D, Bock NA, Leopold DA, Silva AC (2015) Functional  
460 MRI of visual responses in the awake, behaving marmoset. *NeuroImage* 120:1–11.
- 461 Johnston KD, Barker K, Schaeffer L, Cutter DJ, Everling S (2018) Methods for chair restraint  
462 and training of the common marmoset on oculomotor tasks. *J Neurophysiol* 119:1636–  
463 1646.
- 464 Johnston KD, Ma L, Schaeffer L, Everling S (2019) Alpha Oscillations Modulate Preparatory  
465 Activity in Marmoset Area 8Ad. *J Neurosci* 39:1855–1866.
- 466 Knight TA, Fuchs AF (2007) Contribution of the Frontal Eye Field to Gaze Shifts in the Head-  
467 Unrestrained Monkey: Effects of Microstimulation. *J Neurophysiol* 97:618–634.
- 468 Li X, Morgan PS, Ashburner J, Smith J, Rorden C (2016) The first step for neuroimaging data  
469 analysis: DICOM to NIfTI conversion.
- 470 Liu C, Ye FQ, Yen CC-C, Newman JD, Glen D, Leopold DA, Silva AC (2018) A digital 3D  
471 atlas of the marmoset brain based on multi-modal MRI. *NeuroImage* 169:106–116.



- 472 Mitchell JF, Reynolds JH, Miller CT (2014) Active Vision in Marmosets: A Model System for  
473 Visual Neuroscience. *J Neurosci* 34:1183–1194.
- 474 Mott FW, Schuster E, Halliburton WD (1910) Cortical Lamination and Localisation in the Brain  
475 of the Marmoset. *Proc R Soc Lond Ser B Contain Pap Biol Character* 82:124–134.
- 476 Peterson J, Chaddock R, Dalrymple B, Van Sas F, Gilbert KM, Klassen LM, Gati JS, Handler  
477 WB, Chronik BA (2018) Development of a gradient and shim insert system for marmoset  
478 imaging at 9.4 T. In: *Proceedings of the 26th Annual Meeting ISMRM*, pp 4421. Paris,  
479 France.
- 480 Robinson DA, Fuchs AF (1969) Eye movements evoked by stimulation of frontal eye fields. *J*  
481 *Neurophysiol* 32:637–648.
- 482 Russo GS, Bruce CJ (1993) Effect of eye position within the orbit on electrically elicited  
483 saccadic eye movements: a comparison of the macaque monkey's frontal and  
484 supplementary eye fields. *J Neurophysiol* 69:800–818.
- 485 Schall JD (1997) Visuomotor areas of the frontal lobe. In: *Extrastriate cortex in primates*, pp  
486 527–638. Boston, MA: Springer. Available at:  
487 [http://www.psy.vanderbilt.edu/faculty/schall/pdfs/VisuomotorAreasOfTheFrontalLobe-](http://www.psy.vanderbilt.edu/faculty/schall/pdfs/VisuomotorAreasOfTheFrontalLobe-Ch13.pdf)  
488 [Ch13.pdf](http://www.psy.vanderbilt.edu/faculty/schall/pdfs/VisuomotorAreasOfTheFrontalLobe-Ch13.pdf).
- 489 Schlag J, Schlag-Rey M (1987) Evidence for a supplementary eye field. *J Neurophysiol* 57:179–  
490 200.
- 491 Smith SM, Jenkinson M, Woolrich MW, Beckmann CF, Behrens TEJ, Johansen-Berg H,  
492 Bannister PR, De Luca M, Drobnjak I, Flitney DE, Niazy RK, Saunders J, Vickers J,  
493 Zhang Y, De Stefano N, Brady JM, Matthews PM (2004) Advances in functional and  
494 structural MR image analysis and implementation as FSL. *NeuroImage* 23:S208–S219.

- 495 Stanton GB, Deng S-Y, Goldberg EM, McMullen NT (1989) Cytoarchitectural characteristic of  
496 the frontal eye fields in macaque monkeys. *J Comp Neurol* 282:415–427.
- 497 Tomlinson RD, Bahra PS (1986) Combined eye-head gaze shifts in the primate. I. Metrics. *J*  
498 *Neurophysiol* 56:1542–1557.
- 499 Wakabayashi M, Koketsu D, Kondo H, Sato S, Ohara K, Polyakova Z, Chiken S, Hatanaka N,  
500 Nambu A (2018) Development of stereotaxic recording system for awake marmosets  
501 (*Callithrix jacchus*). *Neurosci Res* 135:37–45.
- 502

503 **Figure captions**

504

505 **Fig 1. Evoked motor responses.** (A) Array locations in each marmoset reconstructed using MR  
506 and CT images (see [Localizing the array](#)). (B) Pattern of evoked skeletomotor responses in each  
507 marmoset. (C) Pattern of evoked oculomotor responses in each marmoset. At sites where fixed  
508 vector saccades were observed, mean saccade vector is plotted. Mean saccade vectors were  
509 computed at the minimum current where saccades are evoked at least 75% of the time. Inset  
510 shows small saccade vectors at 2x scale for Marmoset 3. (D) Thresholds for saccades at sites  
511 where saccades were evoked at currents  $\leq 300\mu\text{A}$ .

512

513 **Fig 2. Saccades evoked in FEF sites.** Representative traces for fixed vector saccades in (A)  
514 Marmoset 2 (A), Marmoset 1 (B) and Marmoset 3 (C, D).

515

516 **Fig 3. Saccades evoked in non-FEF sites.** Representative traces for goal-directed saccades from  
517 dorsomedial sites in Marmoset 1 (A) and saccades from rostral sites in Marmoset 2 (B). Open  
518 circles indicate eye position at saccade onset.

519

520 **Fig 4. Current series at representative saccade sites.** Current series at a representative small  
521 (A-C) and large (D-E) saccade sites. Grey bars indicate stimulation train duration. Location of  
522 array sites for series in (A-E) show in (F). (G) Effect of current on proportion of saccades  
523 evoked at all FEF sites in Marmoset 3. (H) Effect of current on saccade latency at low threshold  
524 ( $<50\mu\text{A}$ ) sites in Marmoset 3.

525

526 **Fig 5. Current series at a representative site with staircase saccades.** Arrows indicate median  
527 saccade onset latency. Grey bars indicate stimulation train duration.

528

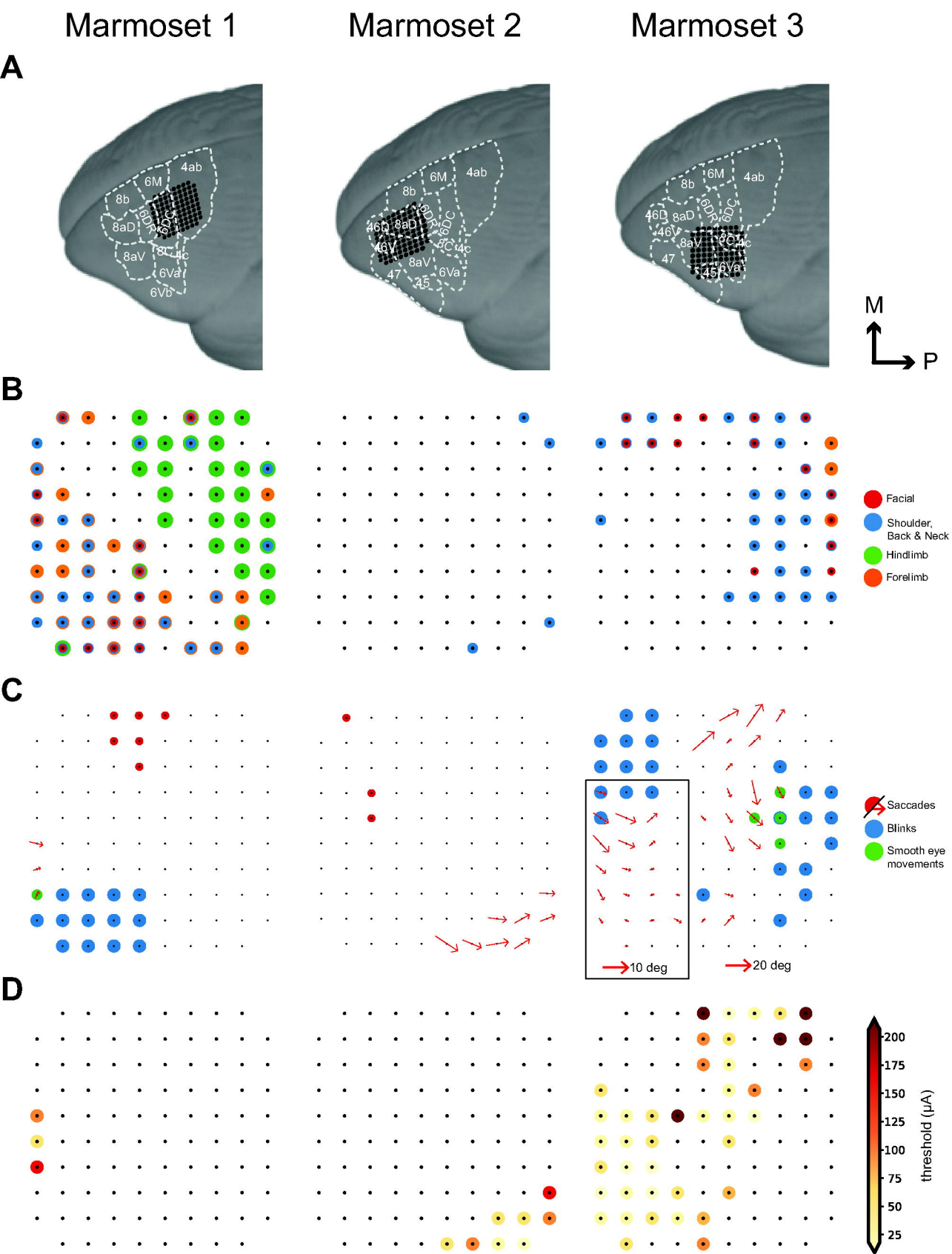
529 **Fig 6. Evoked smooth eye movements.** (A) Smooth eye movement site at 200  $\mu$ A from  
530 Marmoset 1. (B) Current series from a smooth eye movement site in Marmoset 3. Grey bars  
531 indicate stimulation train duration.

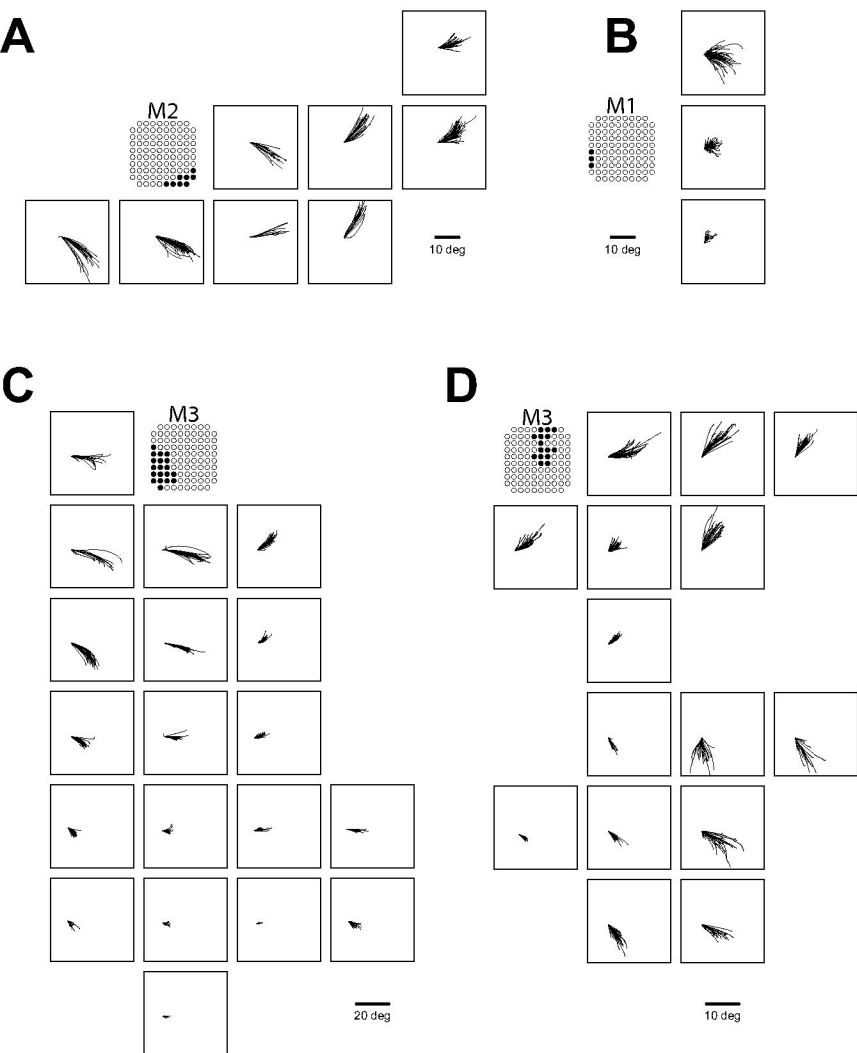
532

533 **Fig 7. Effect of initial eye position.** Saccade traces (above) and effect of initial position on  
534 delta (below) for representative sites from vFEF (A), dFEF (B) and SEF (C). Open circles  
535 indicate eye position at saccade onset. (C) Across all sites, the relationship between  $K_h$  and  $K_v$   
536 values (correlation coefficients from effect of initial eye position analysis) and amplitude. More  
537 negative values indicate a greater effect of initial eye position.

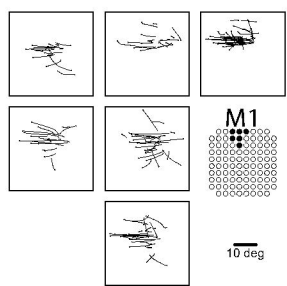
538

539 **Fig 8. Schematic representation of cortical eye fields in marmoset frontal cortex.**





**A**



**B**

